EUROPEAN ORGANIZATION FOR NUCLEAR RESEARCH

CERN/EF 84-11
31 July 1984

INFLUENCE OF THE MAGNETIC FIELD ON THE GATING OF A TIME PROJECTION CHAMBER

S.R. Amendolia[5], W. Blum[4], R. Benetta[1], M. Cherney[7], F. Fidecaro[5], J.P. Froberger[1], B. Hubbard[1(*)], R.C. Jared[7(**)], I. Lehraus[1], F. Liello[6], P.S. Marocchesi[5], R. Matthewson[1], J. May[1], T.C. Meyer[7], E. Milotti[4], F. Nanni[1], A. Peisert[4], M.J. Price[1], F. Ragusa[6], J. Richstein[2], R. Richter[4], L. Rolandi[6], W.D. Schlatter[1], J. Sedgbeer[3], R. Settles[4], U. Stierlin[4], M. Takashima[7], W. Tejessy[1], G. Tromba[6], W. Witzeling[1], Sau Lan Wu[7] and W. Wu[1(***)]

1 CERN, European Organization for Nuclear Research, Geneva, Switzerland
2 Institut für Exp. Phys. IV, University Dortmund, Dortmund, Germany
3 Department of Physics, Imperial College, London, England
4 Max-Planck-Institut für Physik und Astrophysik, München, Germany
5 Dipartimento di Fisica, Sezione INFN and Scuola Normale, Pisa, Italy
6 Instituto di Fisica and Sezione INFN, Trieste, Italy
7 Department of Physics, University of Wisconsin, Madison, Wisconsin, USA(o)

Submitted to Nuclear Instruments & Methods

(*) Now at Department of Physics, University of California, Berkeley, California, USA.

(**) Permanent address: Lawrence Berkeley Laboratory, Berkeley, California, USA.

(***) On leave from the Institute of High Energy Physics, Academia Sinica, Beijing, China.

(o) Supported by the US Department of Energy Contract DE-AC02-76ER00881.

2106F/LR/ed

ABSTRACT

A large cylindrical time projection chamber (TPC 90) with 60 cm diameter, 130 cm driftlength as well as a smaller test-chamber of 30 x 30 x 15 cm^3 have been used to investigate the effects of the magnetic field on the operation of a gated grid. The magnetic field is found to affect strongly the drifting electrons, but not for the positive ions. The results can be well explained by the specific configuration of the combined $\vec{E}$ and $\vec{B}$ fields near the gating grid wires and in the region of the proportional wires.

1. INTRODUCTION

Following the introduction of the time projection chamber (TPC) by D.R. Nygren [1] in 1974 this concept of employing large wireless drift volumes with proportional chambers as endplanes has gained widespread acceptance in high energy physics. The TPC is an attractive device since it is nearly an ideal track detector providing three dimensional track information of high resolution. This feature makes the detector especially suitable for e^+e^- colliding beam experiments in order to investigate complex and rare events.

Operating a large TPC as a continuously sensitive drift chamber, however, can put a severe limitation on its performance with respect to track and momentum resolution: in high background environments positive ions from charge multiplication near the sense wires will eventually move back into the drift space creating (due to their low mobility) track distorting space charges. Also in the proportional cell of the detector itself a high concentration of charge, caused by entering background electrons, will have detrimental effects on the operation (gain) and eventually on the effective lifetime of the chamber [2].

A possible solution for avoiding these problems is the use of a gated grid for controlling the passage of drifting electrons or ions in the TPC. We have investigated this possibility and will show in the following the performance of a gated grid with and without magnetic field.

2. PRINCIPLE OF GATING

The safest and most efficient way to avoid space charges originating in the proportional region is to maintain the TPC insensitive for as long as no suitable event candidate is present. Only in the case of a valid trigger an electronic shutter would be opened and the TPC endplate "exposed" to the event.

One way to achieve this is to use a gated grid, which can be appropriately operated, in order to be totally opaque or transparent to drifting electrons approaching the detection plane of the TPC. Such a

grid located in front of the TPC detection plane, i.e. inside the drift volume, will then be suitably biased to satisfy the above conditions. One can calculate this common potential, denoted by Vg, under the condition that for transparency none of the drift field lines will be absorbed by the gating grid and all will end beyond it on the sense wires. With the specific cell geometry chosen (see fig. 1) the grid becomes transparent for Vg being more negative ($\lesssim$ -70 V) than the fiducial potential at the grid location in drift space.

Then, by making Vg sufficiently positive ($\gtrsim$ 30 V) all drift field lines will finally terminate on the gated grid wires and effectively close the detection plane of the TPC.

Our calculations and measurements show indeed that a gating grid could function properly this way, were it operated in a steady state mode (static operation). However, under realistic conditions the opening and closing of the gate (dynamic operation) must occur fast with respect to the drift time of the electrons.

For the dynamic operation the common voltage Vg would be switched between +30 V and -70 V, thereby inducing severe pickup transients in the sensitive electronics of the chamber. We have rejected this gating scheme, since the recovery time of the electronics would be excessively long.

Instead we have adopted a scheme employed by Breskin et al. [3] and more recently proposed by P. Nemethy et al. [4] to better control effects of high particle fluxes in their detectors. To reduce the pickup problem this gating scheme is based upon the ramping of <u>two</u> opposing voltages, which are symmetrical both in height and time rate of change. To close the grid these two potentials, denoted by $\pm \Delta Vg$, will be applied on neighbouring wires of the grid. The periodic dipole character of the gated grid gives opaqueness to drifting charges and the ramping of opposing voltages results in a strong reduction in electronic pickup. Figs. 2(a,b) illustrate the field configurations for the two modes of gate operation. Thus Vg and $\pm \Delta Vg$ specify completely the conditions of the gated grid.

In this paper we present results of measurements to establish values for Vg and ΔVg. Especially the effect of the magnetic field on the closing of the gated grid will be studied in detail.

3. APPARATUS

The gating tests were performed in two different chambers, both operating at atmospheric pressure. One is smaller (30 X 30 X 15 cm^3), described elsewhere [5], and the other larger with a drift length of 130 cm and a hexagonally shaped wire chamber end plane with a width of 60 cm. This chamber "TPC90" (the magnet bore is 90 cm in diameter) is the test setup for the ALEPH TPC and will be described in another paper.

Both chambers were equipped with similar proportional endplanes and were operated in a magnetic field of up to 1.5 T. They were filled with a gas mixture of argon-methane (90:10) at atmospheric pressure. Before the larger chamber (TPC90) became available, we had investigated the electrostatic gating conditions in the small chamber by directly measuring the electron and ion currents produced by X-ray sources as a function of the gate potentials. These results were verified when TPC90 came into operation. In these later tests the pulse height of tracks produced by a UV Laser was recorded under various gating conditions. In fig. 3 we show a schematic of the basic features of both experimental setups. A difference between the two setups was that in the small TPC a gating grid of 1 mm wire spacing was used, whereas the TPC90 is equipped with a grid of 2 mm spacing. As a consequence different absolute values for the gating parameters Vg and ΔVg were found for the two cases, but relative effects due to the magnetic field were the same. In both setups the average transparency voltage Vg and the closing potentials ± ΔVg were determined for a typical operating environment of the TPC; i.e. E drift ≃ 150 V/cm for the small chamber and E drift ≃ 110 V/cm for TPC90 and gas amplifications between 2 X 10^3 and 4 X 10^4.

4. RESULTS

4.1 No Magnetic Field

In fig. 4 the sense wire (electron) current is plotted versus the common bias Vg for three wire amplifications. From the graphs one can easily deduce that at a positive bias of $Vg \geq 30$ V the transparency of the grid is essentially zero. The plateau value of the curve defines the 100% transparent condition of the gate.

Similar results are shown in fig. 5 for the positive ion current as measured under identical conditions at the central drift electrode. It is remarkable that even under the condition of full gate transparency the ion current accounts for less than 10% of the sense wire current. These remaining positive ions may still produce serious field distortions in the drift volume, and an effective closure of the gate is required to reduce the ion background by two more orders of magnitude. In fig. 6 we show the effect of a symmetric potential $\pm \Delta Vg$ around the common gate bias $Vg = -100$ V:

$$V^+ = Vg + \Delta Vg$$

$$V^- = Vg - \Delta Vg$$

Note that with $V^+ = V^- = -100$ V the grid is fully transparent for drifting electrons.

The steep slope of the graph illustrates, how effectively the dipole field of the gating grid reduces the charge due to gas amplification near the sense wires down to the level of primary ionization in the drift region.

In summary, without magnetic field a gating grid of 1 mm wire pitch fulfils the condition of transparency at $Vg \leq -100$ V and $\Delta Vg = 0$, and opaqueness at $\Delta Vg = \pm 20$ V.

4.2 With Magnetic Field

The small TPC was consequently placed in a spectrometer magnet at the CERN SPS, where the gating could be tested with fields as high as 1.5 T. For technical reasons the electron current could not be measured. As the data in fig. 7 in comparison with fig. 6 indicate, the magnetic field of 1.5 T has essentially no influence on the positive ion feedback into the drift volume.

As soon as the TPC90 became available the gating in a magnetic field could be investigated again with 2 mm gating-wire pitch. One would expect that doubling the pitch would mean in increase in ΔVg by a factor of two as well, to ± 40 V, in order to close the gated grid. This is indeed the case without magnetic field, as confirmed by measurements done by recording the pulseheight of laser tracks drifting through the grid.

As the magnetic field is increased, however, the grid again becomes transparent to electrons, unless ΔVg is raised accordingly. This behaviour is illustrated in fig. 8. Thus to compensate for the effect of a given magnetic field the voltage step ΔVg has to be adjusted to ΔVg^{max} to close the gate again.

In fig. 9 we show the systematic behaviour of ΔVg^{max} for various magnetic fields. The error bars indicate the uncertainty in ΔVg^{max} due to the fact that the laser signal approaches the noise level of the electronics.

5. NUMERICAL ESTIMATES

For the understanding of the gating in a magnetic field we must recall the specific electric field configuration near the gating grid in figure 2(b) (closed condition).

Without magnetic field, all electrons following strictly the electric field lines, which start at the central field electrode and terminate at the gating grid, cannot traverse this grid. In the presence of a magnetic field the motion of electrons is no longer governed by the electric field alone but by both fields through the expression [6]:

$$\vec{v} = \frac{\mu}{1 + \omega^2\tau^2}\left(\vec{E} + \frac{\vec{E} \times \vec{B}}{|B|}\,\omega\tau + \frac{(\vec{E} \cdot \vec{B})\vec{B}}{B^2}\,\omega^2\tau^2\right) \qquad (1)$$

with

μ (mobility)

$\omega = \frac{eB}{me}$ (cyclotron frequency)

$\tau = \tau(E)$ (mean collision time)

$$\vec{B} = [0,\ 0,\ B_z] \qquad (2)$$

The coordinate system used here is the z-axis is normal to the wire plane and the x-component parallel to it, but normal to the wire direction. One can choose a field point E(x,z), such that:

$$\vec{E} = [E \cdot \cos\alpha,\ 0,\ E \sin\alpha] \qquad (3)$$

where α defines the angle between E(x,z) and the positive x-direction of the wire plane. Expressions (1) to (3) will then lead to:

$$v_x = \frac{\mu E \cos\alpha}{1 + \omega^2\tau^2} \qquad (4)$$

$$v_y = \frac{\mu E \cos\alpha\ \omega\tau}{1 + \omega^2\tau^2} \approx \frac{\mu E \cos\alpha}{\omega\tau} \qquad (5)$$

and

$$v_z = \frac{\mu E \sin\alpha\ \omega^2\tau^2}{1 + \omega^2\tau^2} \approx \mu E \sin\alpha \qquad (6)$$

In the x-z-plane the trajectories of moving charges are defined by

$$\tan\psi = \frac{v_z}{v_x} = \frac{E_z}{E_x} \cdot (\omega\tau)^2$$

$$= \tan\alpha \cdot \omega^2\tau^2$$

With $\omega\tau >> 1$ ($\psi \to 90°$), the electric charges follow essentially the B-field lines and ignore the electric field of the closed grid. The larger the $\omega\tau$-value, the more electrons have the tendency to traverse the grid.

We have made independent measurements of $\omega\tau$ as a function of E and B [7] and find for normal conditions in the drift volume, B = 1.2 T and E = 110 V/cm, $\omega\tau \approx 8$. Given the measured dependence of $\omega\tau$ on E, we can

calculate the particle trajectories from eqs (4) and (6) in the vicinity of the grid, and the result is shown for 2 values of ΔVg, ± 50 V and ± 70 V, in fig. 8. The calculation is seen to agree with the measured values.

Unlike electrons the positive ions, which travel back from the sense wires towards the gating grid, acquire a small $\omega\tau$-value due to their very low mobility. Therefore the ions follow entirely the electric field lines while moving towards the gated grid and do not penetrate it.

5. CONCLUSION

We have studied the operation of a gated grid in two TPC's, one small and one large. These chambers are tests for the ALEPH TPC for which the operating conditions (atmospheric pressure and high B) have been chosen for optimum spatial resolution by taking advantage of the damping action of a large $\omega\tau$, to reduce transverse diffusion. The gating data of the test chamber can be well explained with our knowledge of $\omega\tau$ near the gating grid wires; i.e. they prove that the operation of a dipole gating grid in the presence of a magnetic field is different for electrons and ions due to their specific $\omega\tau$-value. Under the stringent requirement that neither positive ions escape into the drift volume nor electrons enter the TPC endplane, dipole-gating voltages exceeding $\Delta Vg = \pm 190$ V would be needed to close the grid at B = 1.5 T for 2 mm wire spacing.

If background conditions permit, the gating voltage could be relaxed to the extent that the drift region is kept free of positive ions inspite of electrons penetrating the gate. Finally, the different effect of the gated grid on electrons and positive ions may open new interesting possibilities by actually making use of this DIODE characteristic of the gated detector.

Acknowledgements

We would like to thank the technical division of the Max Planck Institut für Physik und Astrophysik in Munich, the EF-Instrumentation group, as well as the PS generator group at CERN for their technical support. The help of the NA1 Collaboration for letting us use their spectrometer magnet is also very much appreciated.

REFERENCES

[1] D.R. Nygren, Proposal to investigate the feasibility of a novel concept in particle detection, LBL internal report, February 1974.

[2] J. Adam et al., A study of ageing effects in wire chambers, Nucl. Instr. and Methods, 217 (1983), 291 and

H. Sipila and M.L. Jarvinen, Extended lifetime of a wire chamber, Nucl. Instr. and Methods 217 (1983) 298.

[3] A. Breskin et al., High flux operation of the gated multistep avalanche chamber, Nucl. Instr. and Methods 178 (1980) 11.

[4] P. Nemethy, P.J. Oddone, N. Toge and A. Ishibashi, Gated time Projection Chamber, LBL internal report 15281, November 1982.

[5] S.R. Amendolia et al., E x B and angular effects in the avalanche location along the wire with cathode pad readout, Nucl. Instr. and Methods 217 (1983) 317.

[6] W.P. Allis, Motion of electrons and ions, Handbuch der Physik, Vol. XXI.

[7] S.R. Amendolia et al., Calibration field inhomogeneities in a Time Projection Chamber with laser rays, Topical Seminar on e^+e^- Instrumentation, San Minato, Italy, 21-25 May 1984.

FIGURE CAPTIONS

Fig. 1 Geometry of proportional cell.

Fig. 2 (a) Electric field configuration with gated grid transparent.
(b) Electric field configuration with gated grid opaque.

Fig. 3 Schematic of experimental setup.

Fig. 4 Electron Current vs. Vg - transparency curve for electrons for three different sense-wire voltages.

Fig. 5 Ion current vs. Vg - transparency curve for positive ions for three different sense-wire voltages.

Fig. 6 Transparency for positive ions as a function of ΔVg - without magnetic field.

Fig. 7 Transparency for positive ions as a function of ΔVg with magnetic field.

Fig. 8 Transparency for electrons vs. ΔVg for various magnetic fields.

Fig. 9 Closing voltage ΔVg^{max} as a function of magnetic field.

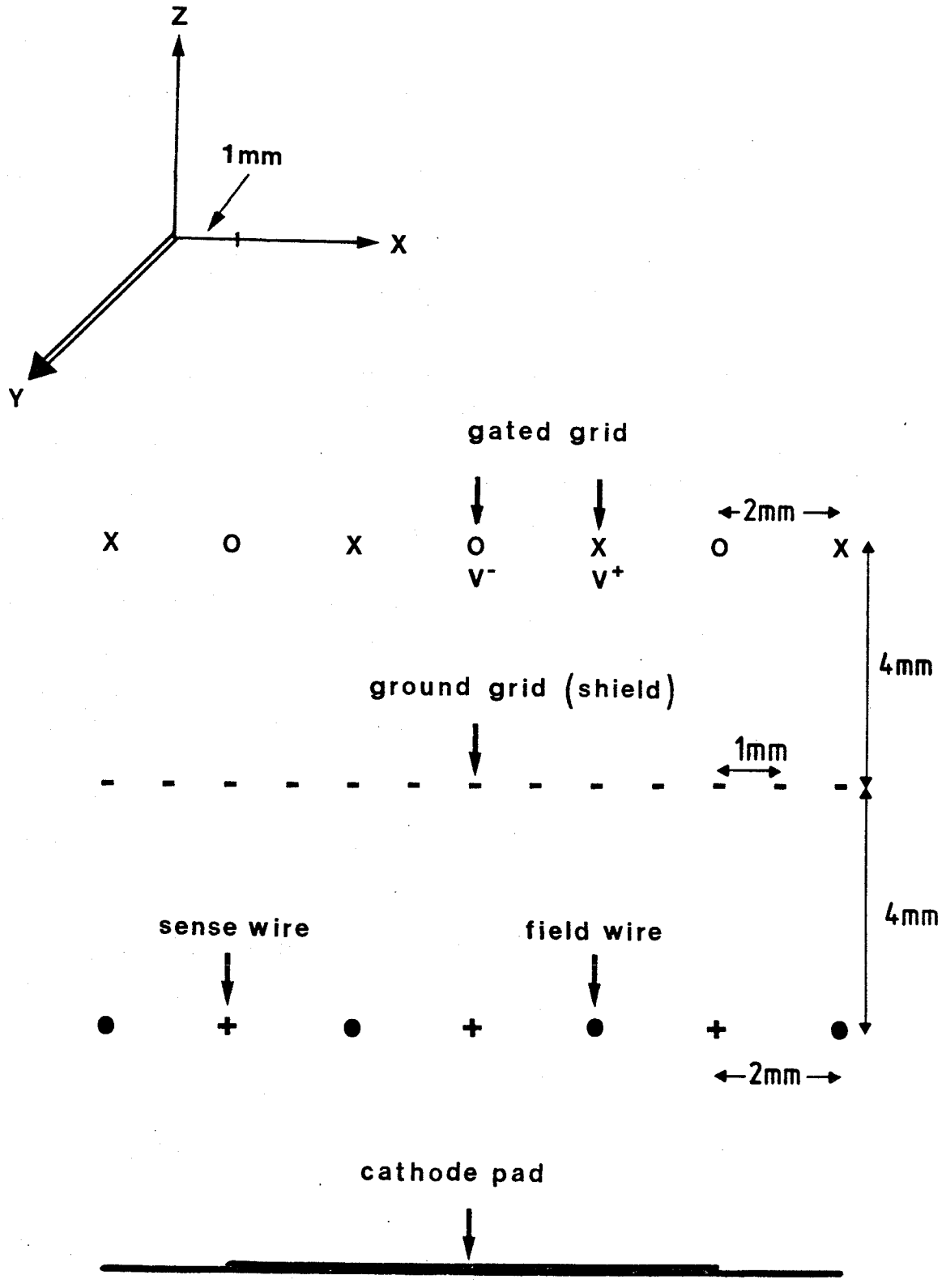
Z
1mm
X
Y
gated grid
2mm
X
O
X
O
V⁻
X
V⁺
O
X
4mm
ground grid (shield)
1mm
4mm
sense wire
field wire
2mm
cathode pad

FIG .1

OPEN AND CLOSED GRID CONFIGURATIONS

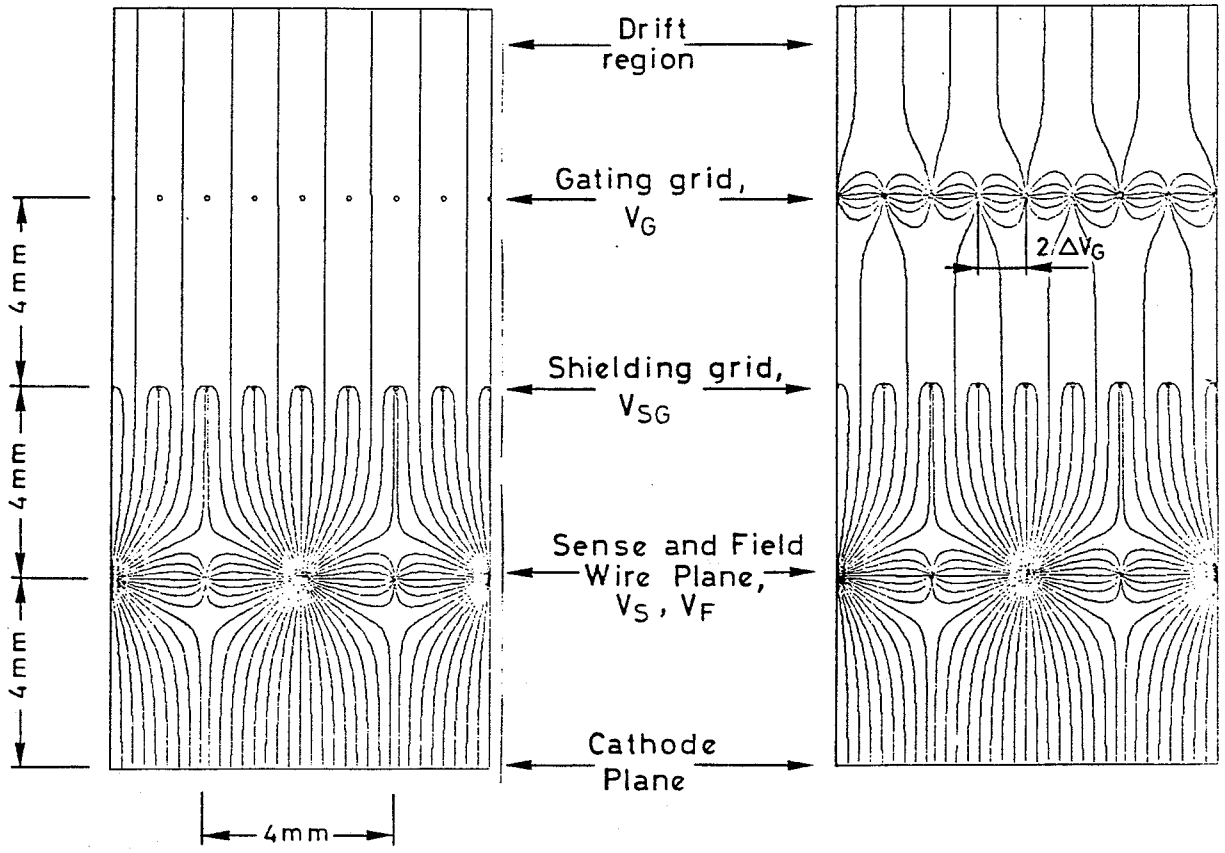

FIG. 2

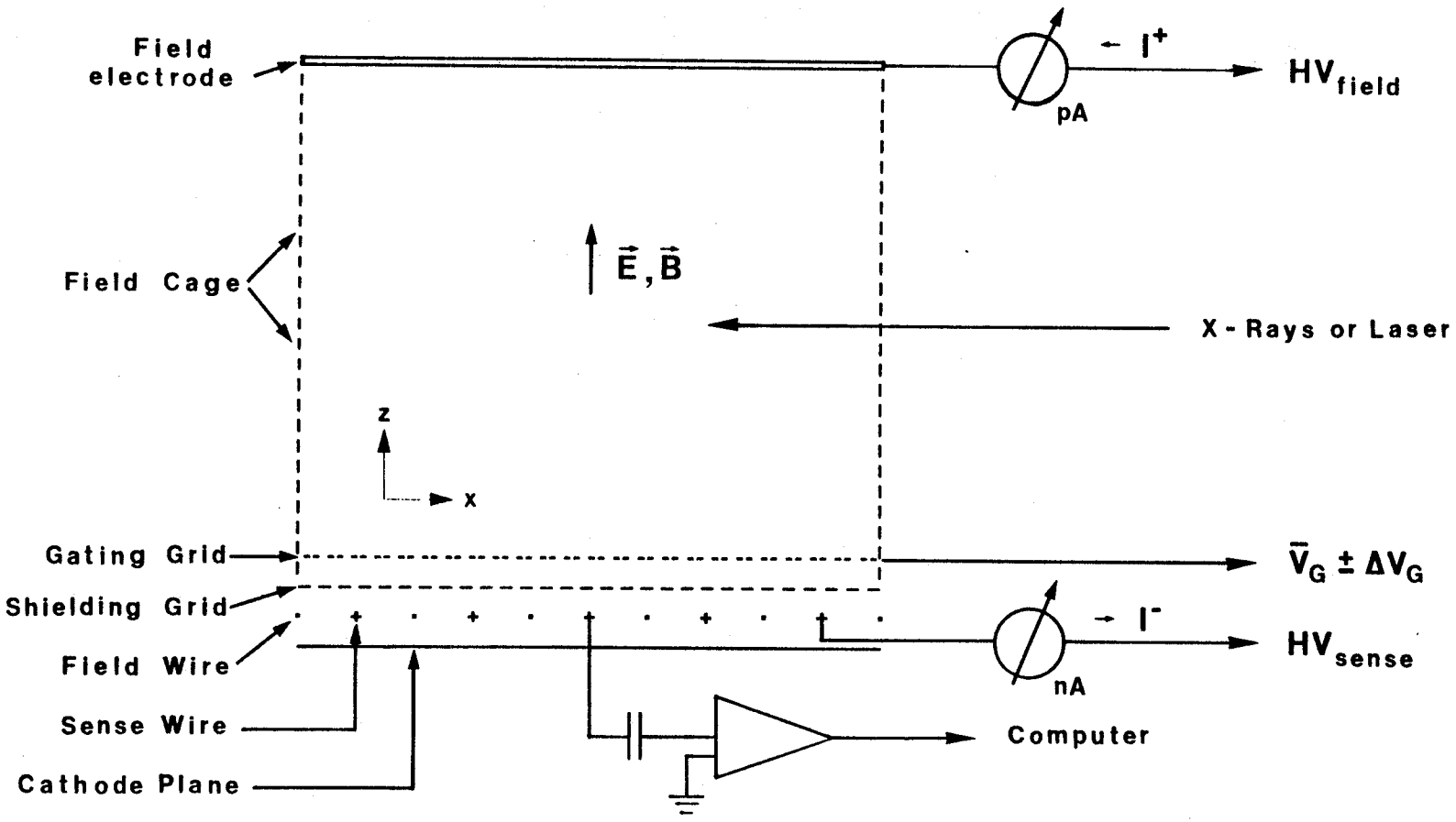
Field electrode
- I+
pA
HV field
Field Cage
E, B
X - Rays or Laser
z
x
Gating Grid
V̄G ± ΔVG
Shielding Grid
- I-
HV sense
Field Wire
nA
Sense Wire
Computer
Cathode Plane

FIG. 3

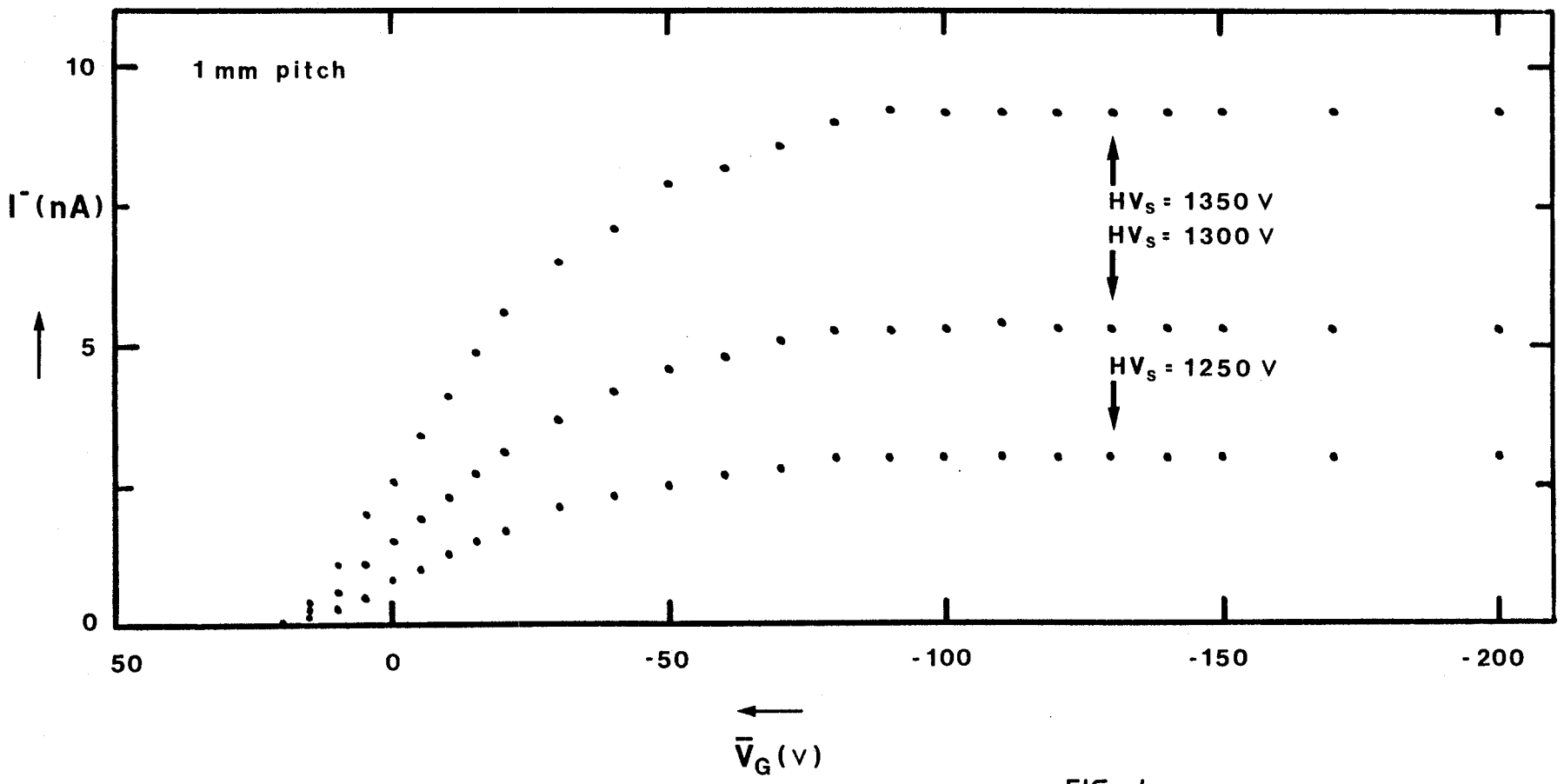
1 mm pitch
10
5
0
I⁻(nA)
HVs = 1350 V
HVs = 1300 V
HVs = 1250 V
50
0
-50
-100
-150
-200
V̄G(V)

FIG. 4

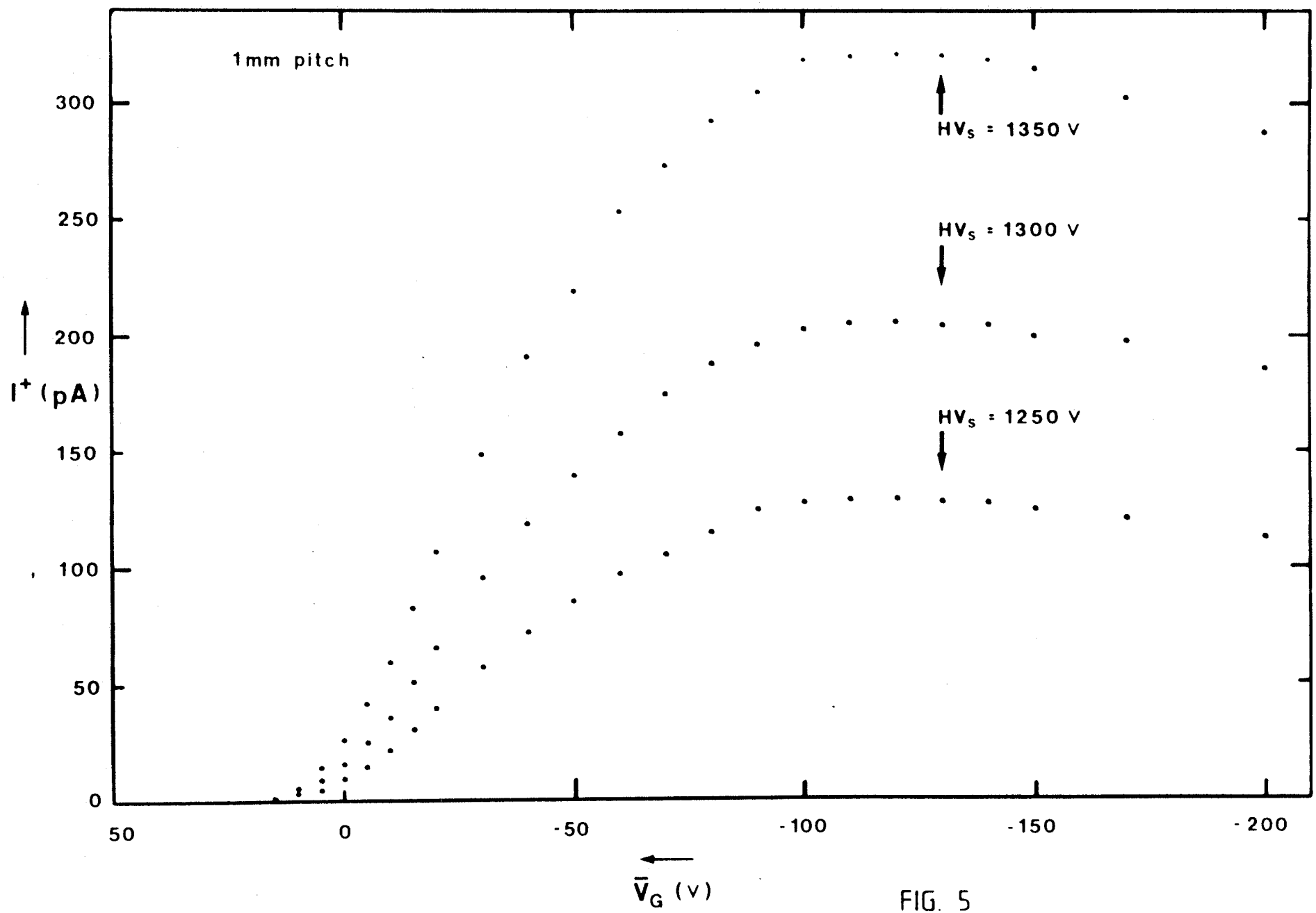
1mm pitch
300
250
200
150
100
50
0
I+ (pA)
HVs = 1350 V
HVs = 1300 V
HVs = 1250 V
50
0
-50
-100
-150
-200
V̄G (V)

FIG. 5

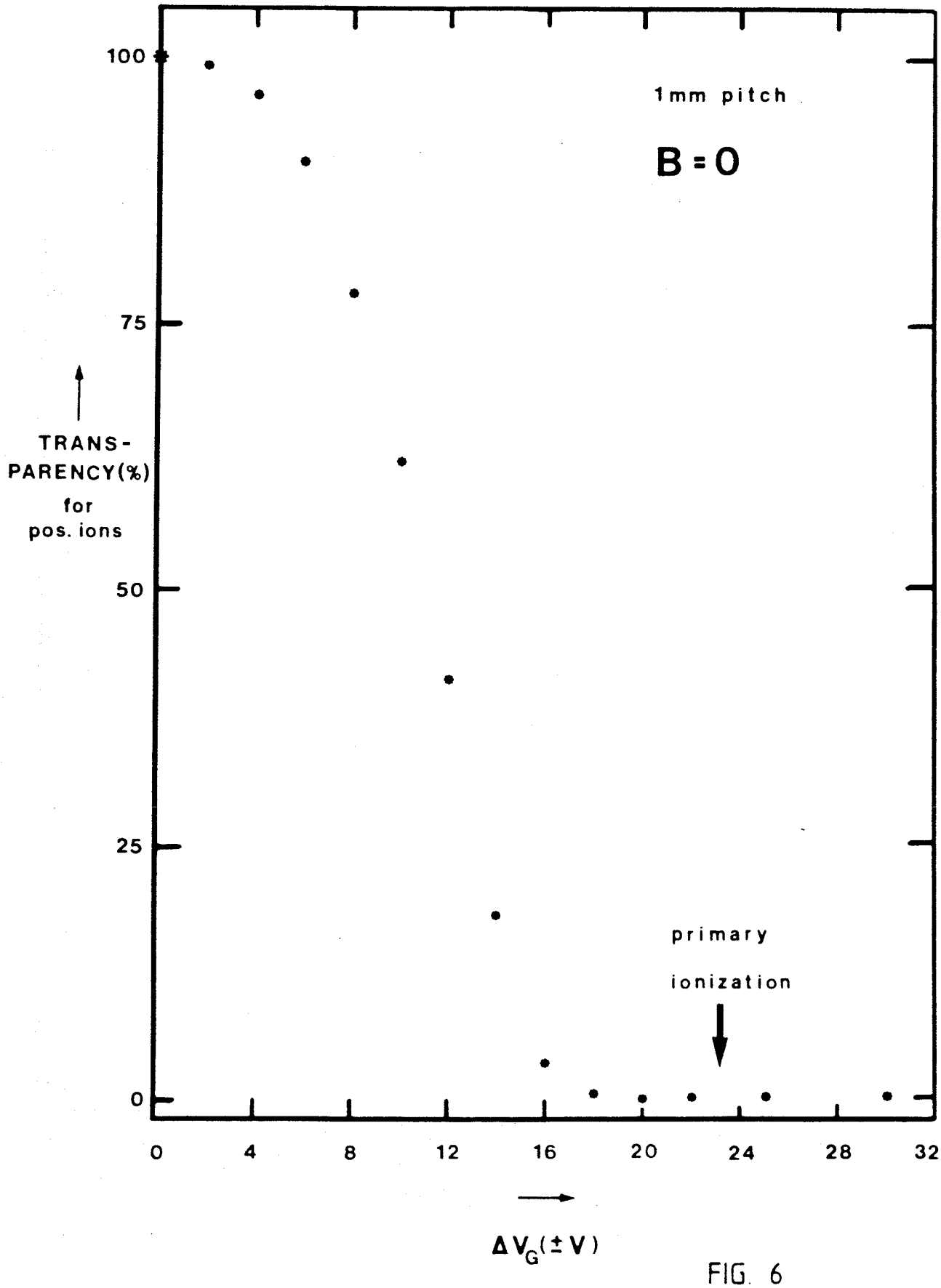
100
75
50
25
0
1mm pitch
B = 0
TRANS-
PARENCY(%)
for
pos. ions
primary
ionization
0
4
8
12
16
20
24
28
32
ΔV_G(±V)

FIG. 6

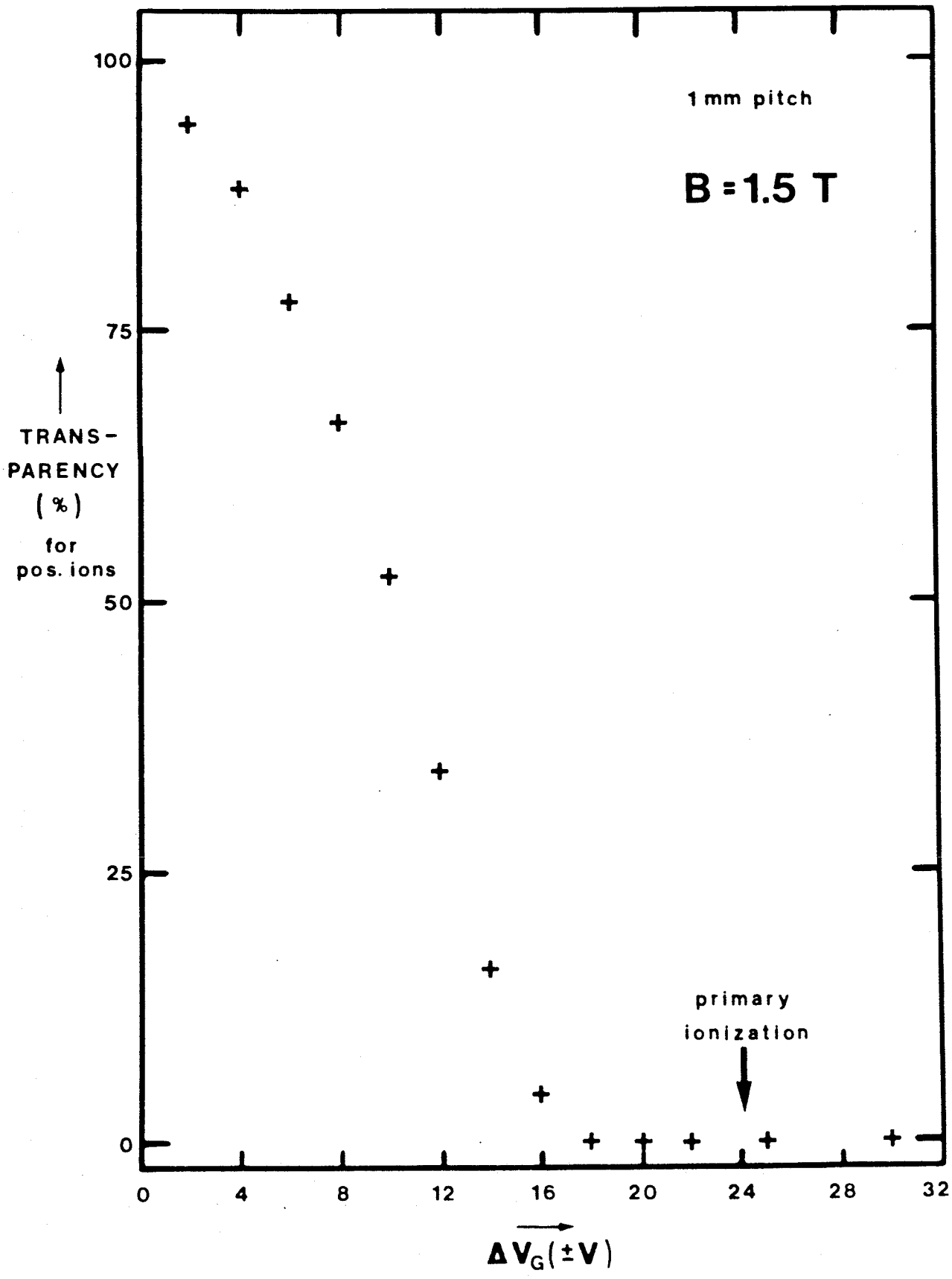
100
75
50
25
0
1 mm pitch
B = 1.5 T
TRANS-
PARENCY
(%)
for
pos. ions
primary
ionization
0
4
8
12
16
20
24
28
32
ΔV_G(±V)

FIG. 7

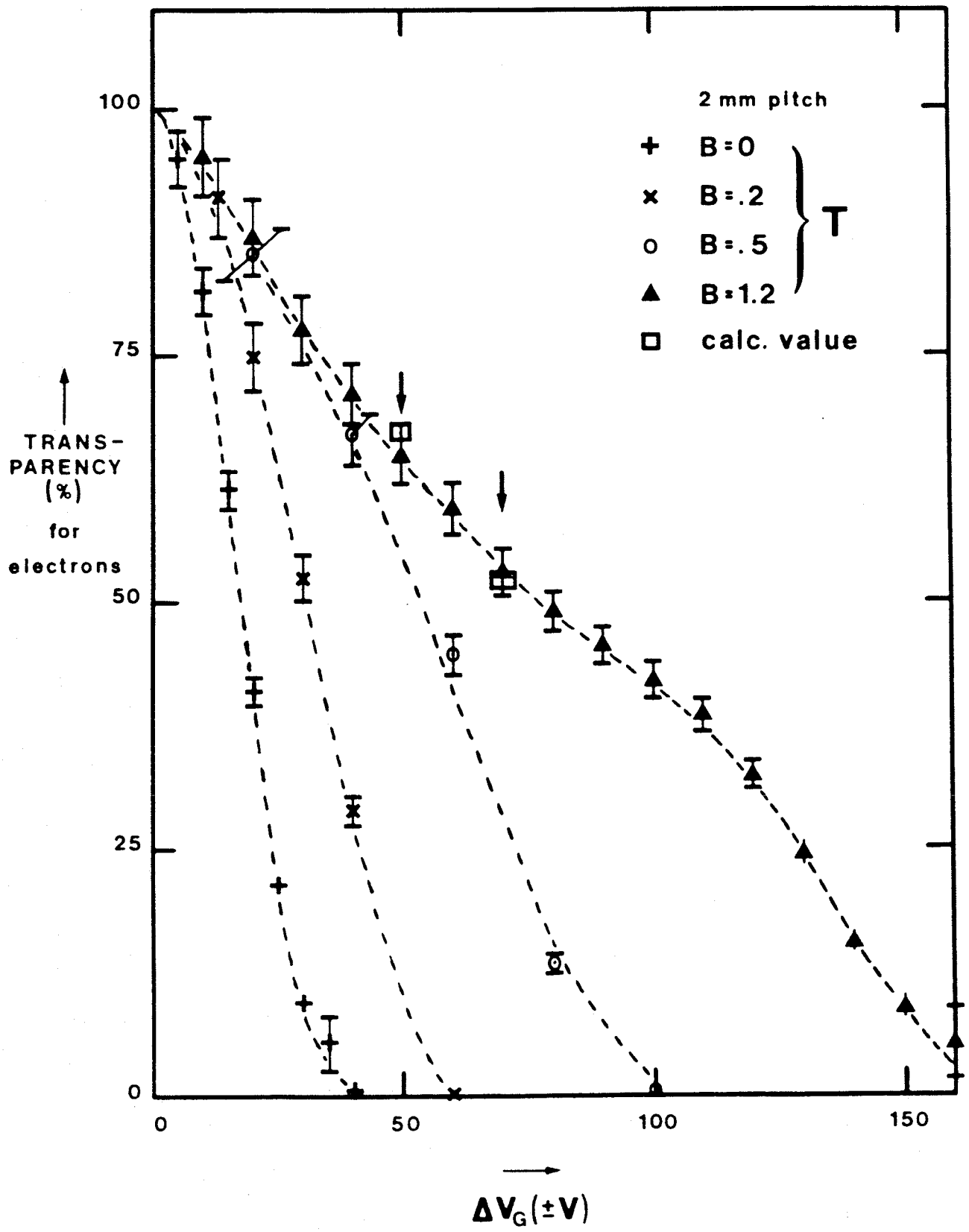
2 mm pitch
B=0
B=.2
B=.5
B=1.2
T
calc. value
100
75
50
25
0
TRANS-
PARENCY
(%)
for
electrons
0
50
100
150
ΔV_G(±V)

FIG. 8

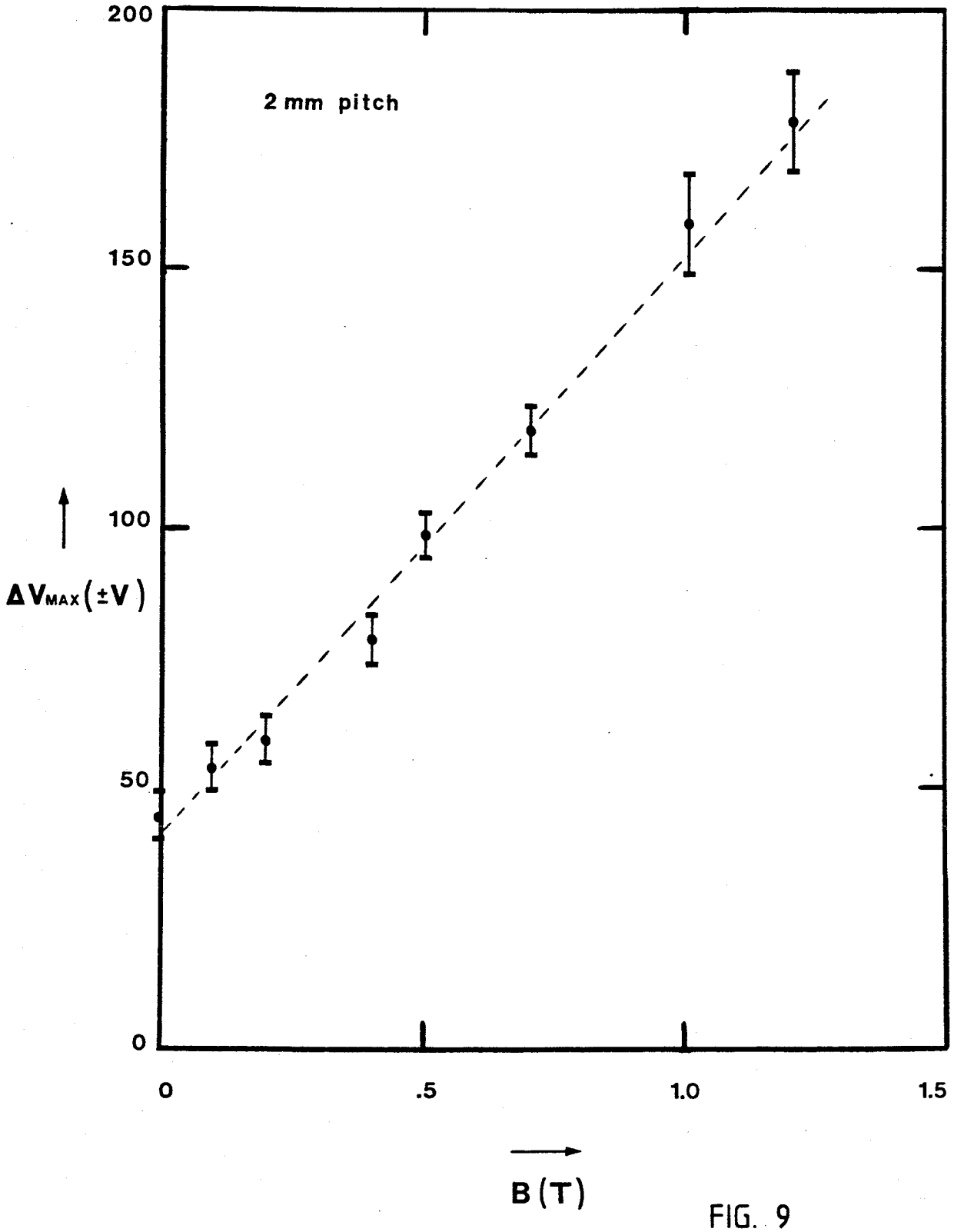

FIG. 9